Exploring the low temperature tempering range of low alloy quenched and tempered steels

Available online at www.sciencedirect.com

ScienceDirect

Procedia Structural Integrity 18 (2019) 703–710

Structural Integrity Procedia

www.elsevier.com/locate/procedia

25th International Conference on Fracture and Structural Integrity

Exploring the low temperature tempering range of low alloy quenched and tempered steels

D. Firrao[a,*], P. Matteis[a], A. De Sario[b]

[a]*Politecnico di Torino, Corso Duca degli abruzzi 24, Torino, It-10129, Italy*
[b]*Vimi Fasteners S.p.A., Via Labriola 19, Novellara, It-42017, Italy*

Abstract

It is well known that quenched and tempered alloy steel components with ultimate tensile strength in excess of 1400 MPa are seldom employed as mechanical components, due to their not adequate ductility, as ascertained by multiple researches performed during World War II and soon after. Nevertheless, use of low temperature tempered steels in some niche applications, as well as researches performed on surface heat treated high carbon steels and on their behavior upon tempering in the vicinity of 200°C have stemmed into renewed interest in quenched and low temperature tempered low alloy steels. Application to 36NiCrMo16 steel bars is examined here, by means of tensile and hardness tests and fractographic and metallographic examinations after quenching and tempering in the 160 to 440 °C temperature range.

Peer-review under responsibility of the Gruppo Italiano Frattura (IGF) ExCo.

Keywords: High strenght steels; low temperature tempering.

1. Introduction

Researches published in USA just after World War II on low alloy quenched and tempered steels have shed a negative light on the use of low alloyed steels in the medium to low temperature tempering regime, where they reach UTS values well above 1400 MPa (Sachs et al., 1950) which was since then considered for a long time the limiting safe tensile strength in mechanical machines.

* Corresponding author.
E-mail address: donato.firrao@formerfaculty.polito.it

2452-3216
Peer-review under responsibility of the Gruppo Italiano Frattura (IGF) ExCo.
10.1016/j.prostr.2019.08.218

There have been, however, several niche application of quenched and low-temperature tempered steels, especially for wear resistance (Dudzinski et al, 2008), armor (Borvik et al., 2009), and car safety (Karbasian and Tekkaya, 2010).

Better assessment of stress and strain distribution in joining steel components and the everlasting quest for higher and higher strengths to reduce mass in critical applications, urge to revisit the whole field of medium to low tempering temperatures to set a not too daring UTS limit to be used by mechanical engineers in their new designs.

In such range of tempering temperatures, quenched steel microstructures change, as mainly studied by M. Cohen and his co-workers at MIT (Averbach and Cohen, 1949, Roberts et al., 1953, Mentser, 1959, Cohen, 1983), yielding cubic martensite (0.3% C) and ε-carbides - now termed conversion carbides (Krauss, 1984, Lee and Krauss 1992).

Tests performed by the senior author while investigating induction hardening and low temperature tempering of UNI 88MnV8KU tool steel (similar to ISO 90MnCrV8 and AISI O2) constitute the starting point of a new research program aiming to fully assess a safe use of ultra high strength steels.

In the case of 88MnV8KU steel, a peaking of impact resistance was ascertained at 210 °C tempering temperature, with only a reasonably low loss of hardness in respect to the as quenched steel (figure 1).

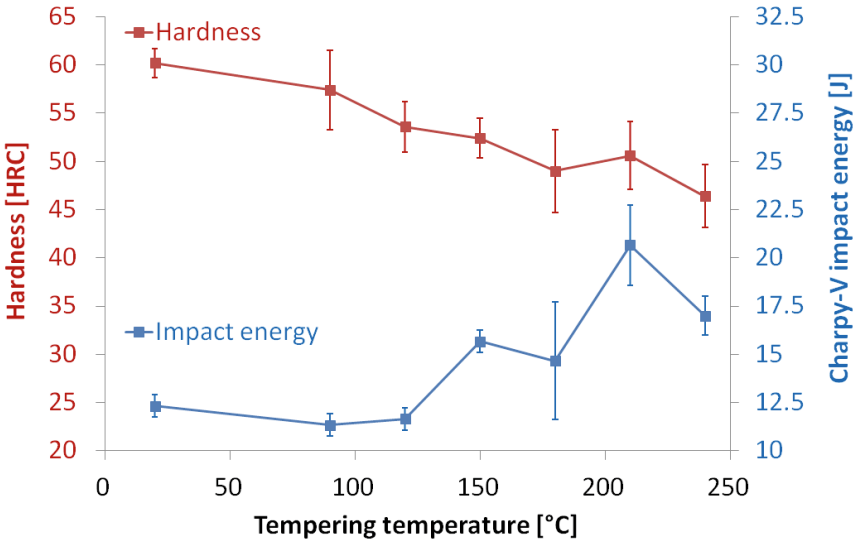

Fig. 1. Impact energy and hardness of quenched and tempered 88MnV8KU tool steel.

The use of a steel more suitable for mechanical apparatuses has induced to repeat low tempering tests on a medium carbon, low alloy Ni-Cr-Mo quenched steel, namely 36NiCrMo16 (compliant to the EN 10083 European standard), where the use of a high Ni content should counteract the low ductility imparted by the presence of cubic martensite in the steel microstructure.

2. Experiments

36NiCrMo16 steel, 20 mm diameter bars were received in the spheroidized annealed metallurgical state, with the following composition (optical emission spectroscopy, mass %): C 0.36, Ni 3.7, Cr 1.7, Mo 0.28, Mn 0.53, Cu 0.49, Si 0.29, S 0.012, P 0.012, Al 0.026, V 0.011, Nb 0.005, B 0.0005.

Cylindrical specimens with 11 or 17 mm diameter were machined from the bars and heat treated, with the following steps: cleaning; austenitizing at 900 °C for 60 min; quenching in agitated oil at 60 °C; cleaning; tempering for 60 min at increasing temperatures in the 160 to 440 °C range.

The heat treated specimens were characterized by means of optical microscopy, hardness and tensile testing.

Several tensile samples were tested for each condition, with 9 or 10 mm calibrated diameter and proportional gage length (equal to 5 times the diameter). In particular, at least 10 tensile specimens with 10 mm diameter were tested for each of the following tempering temperature: 160, 180, 200 and 440 °C, whereas 2 tensile specimens with 10 mm diameter and one tensile specimen with 9 mm diameter were tested for each of the following tempering temperatures: 220, 240, 320, 400 and 420 °C. In most cases, the yield stress was measured qualitatively on the test autographic record, causing a relatively large scatter and uncertainty.

Finally, representative broken tensile specimens were subjected to fractographic analysis by means of electron microscopy and energy dispersion spectroscopy.

3. Results

The steel microstructure after quenching was fully martensitic, with slight chemical segregation (figure 2a); its evolution upon tempering up to 440 °C is shown in Figs. 2b to 2d.

Microstructure variations are not evident in the optical microscopy examinations up to the 200 °C tempering temperature; in contrast, at 440 °C features become sharper and the evolution from a mainly martensitic structure to a ferrite-spheroidal cementite one is evident.

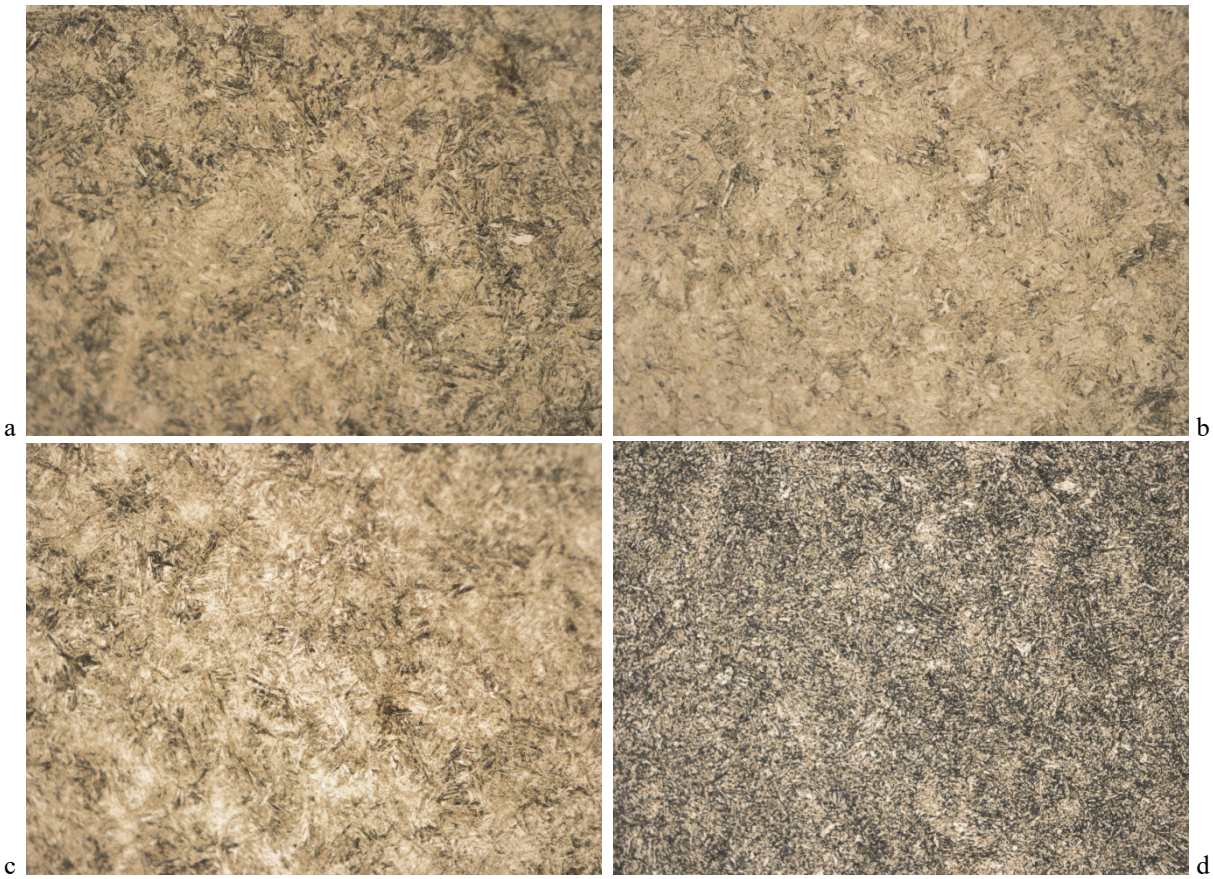

Fig. 2 - Steel microstructure after quenching (a) and after tempering at 160 °C (b), 200 °C (c), and 440 °C (d). Nital etching. Original magnification: 500 x.

The mechanical properties at room temperature, as a function of the tested tempering temperature, are illustrated in figure 3. The quenched and tempered material exhibits its maximum strength after tempering at about 180 °C, even if at this temperature the hardness is somewhat lower than at 160 or 200 °C; whereas, by increasing the tempering temperature above 200 °C both strength and hardness show a marked decrease tendency. The trend of the yield stress is similar to that of the ultimate tensile strength, except that its peak value is probably closer to 240 °C. In contrast, the ductility (or elongation at fracture) and the reduction of area at fracture increase steeply with the tempering temperature below 220 °C, and thereafter exhibit only smaller variations up to the higher examined tempering temperature (440 °C).

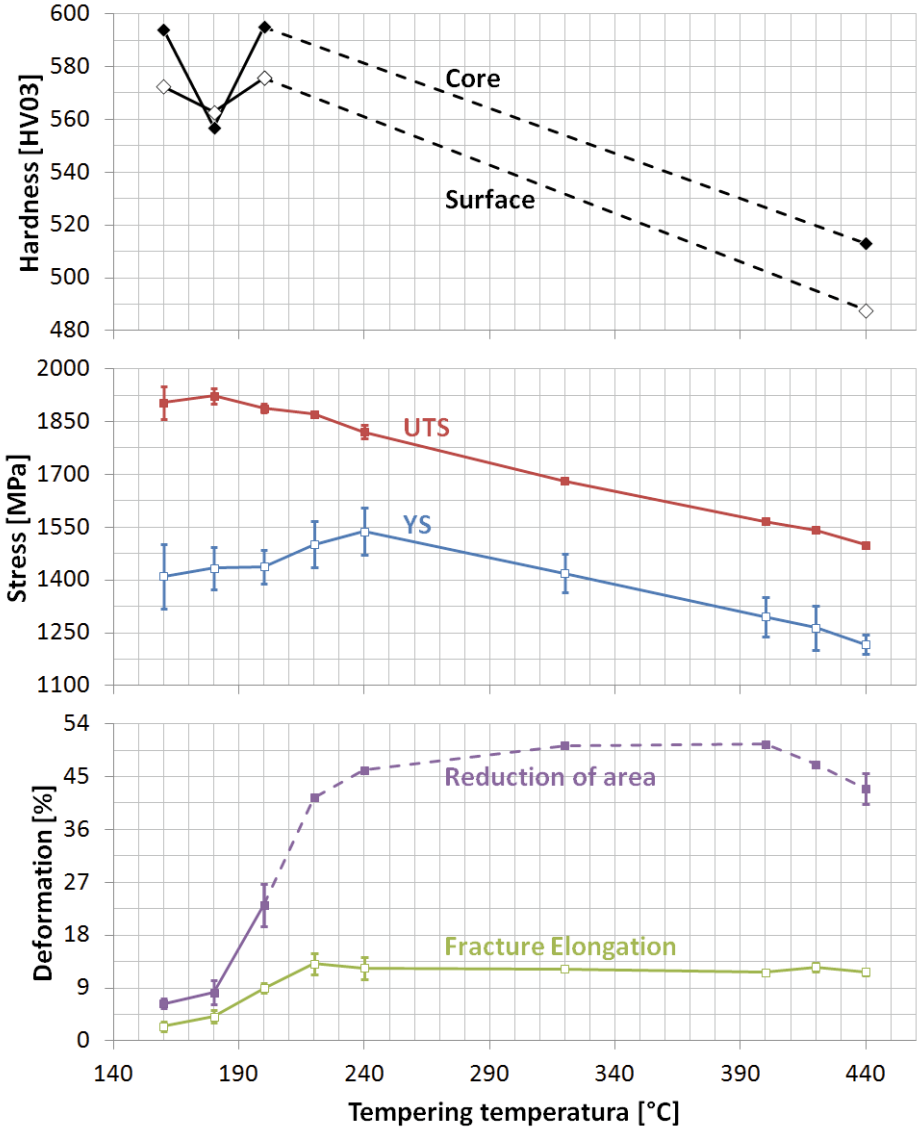

Fig. 3 - Steel mechanical properties (at room temperature) as a function of the tempering temperature. Hardness at the specimen surface (mean value in a 1 mm layer) and core; ultimate tensile strength; yield stress; reduction of area; and elongation at fracture. All core hardness data points and the reduction of area data points between 220 and 420 °C are individual test points; all other data points are mean values. Vertical bars represent the standard deviation.

The tensile fracture surface in all cases exhibits the well known cup-and-cone morphology, figure 4. The conical region becomes larger by increasing the tempering temperature, but its microscopic fracture mechanism does not change, always exhibiting shallow and oriented dimples, formed by ductile shearing.

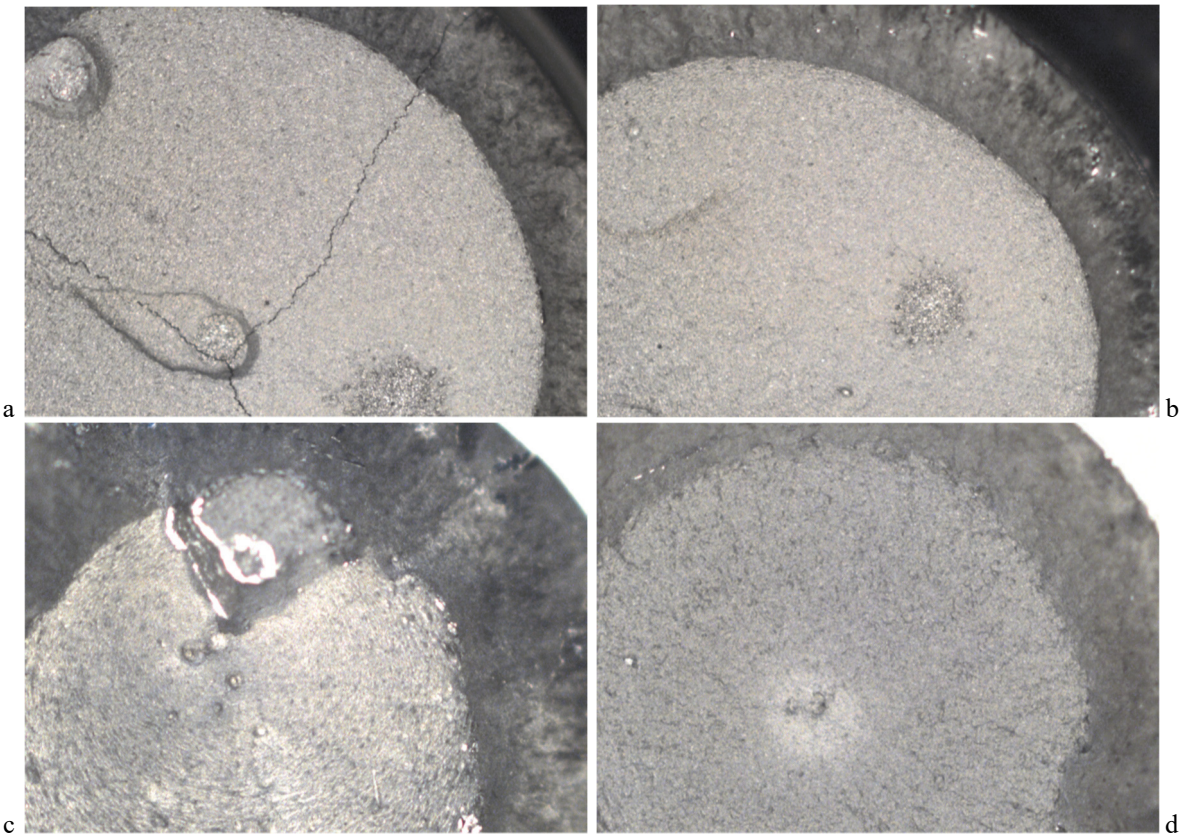

Fig. 4 - Fracture surfaces of tensile specimens tempered at 160 °C (a), 180 °C (b), 200 °C (c) and 440 °C (d). Low magnification optical microscopy.

In the central region (Figs. 5 to 9) the prevalent fracture mode is always microvoid coalescence, with shallow and homogeneous dimples confined on a flat and smooth fracture plane at the lower tempering temperatures (figure 5a), gradually evolving towards deeper and inhomogeneous ones forming a much rougher overall surface at the higher tempering temperature (Fig 8 and 9).

The fracture surfaces formed after low temperature tempering at 160 °C also exhibit in their central region secondary cracks (figure 5b) and large brittle islands (figure 5c, d); by increasing the tempering temperature at and above 180 °C, secondary cracks do not occur anymore, but several small and large brittle islands occur after tempering at 180 and 200 °C, mostly lying above or below the mean fracture plane and thus resulting in a more complex fracture path (figures 6a and 7a). None of these features occurs after tempering in the 220 to 440 °C range (figure 8 and 9).

The fracture mechanism close to the secondary cracks and inside the brittle islands is mostly intergranular after tempering at 160 °C (figure 5b, d), it is quasi-cleavage after tempering at 200 °C (figure 7), and it is mixed (intergranular and cleavage) after tempering at 180 °C. The brittle islands seem to irradiate from point defects, which may be strings of submicrometric inclusions causing first a small crack, then a blunting region, and finally the whole brittle islands (figures 5c and 7b). Only in one instance a large spherical inclusion, with about 40 μm diameter, consisting of aluminum, calcium and magnesium oxides, was detected on the fracture surface (figure 7c, d).

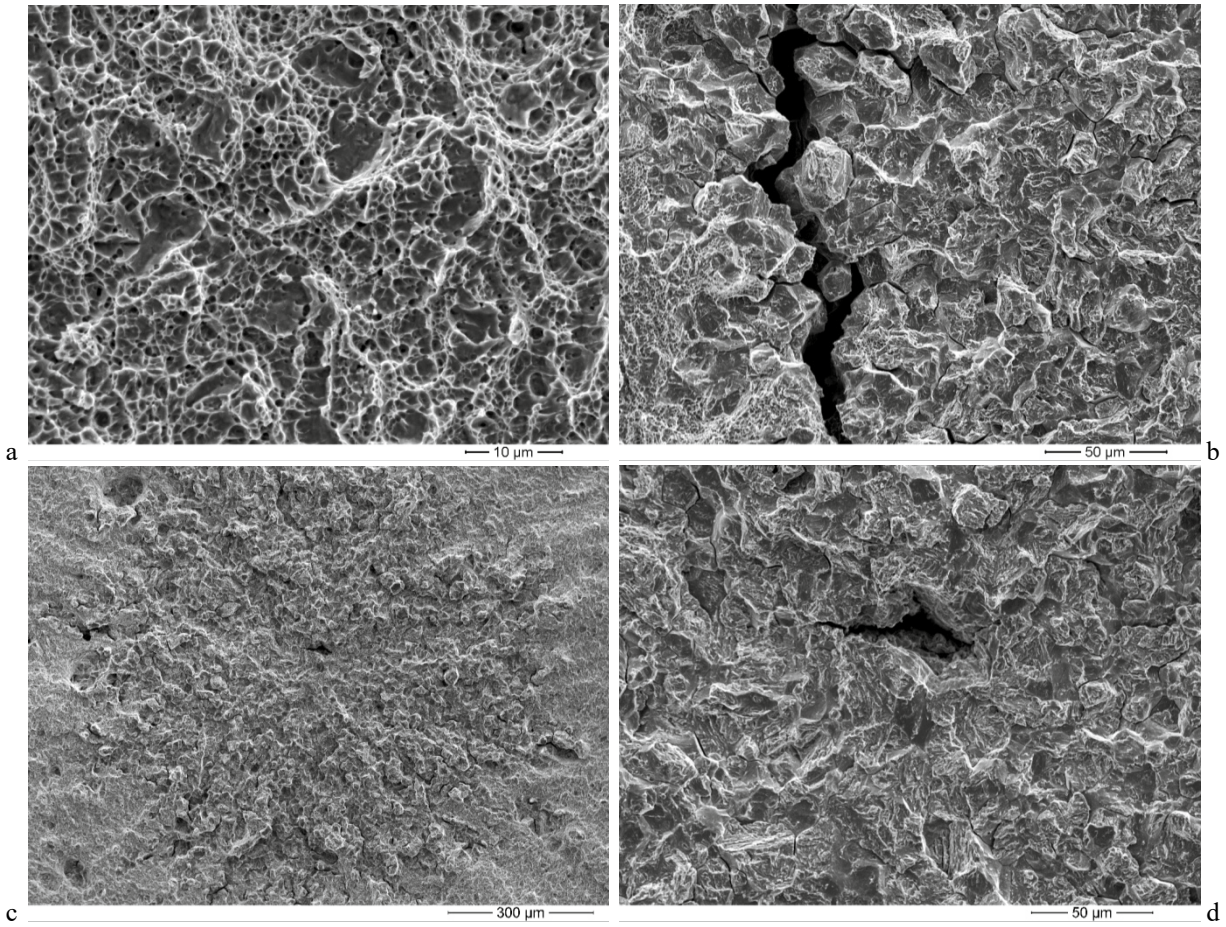

Fig. 5 - Fracture surface of a tensile specimen tempered at 160 °C. Electron microscopy. Central (normal) part. Prevalent ductile fracture mechanism (a); secondary crack (b); brittle fracture island (c, d).

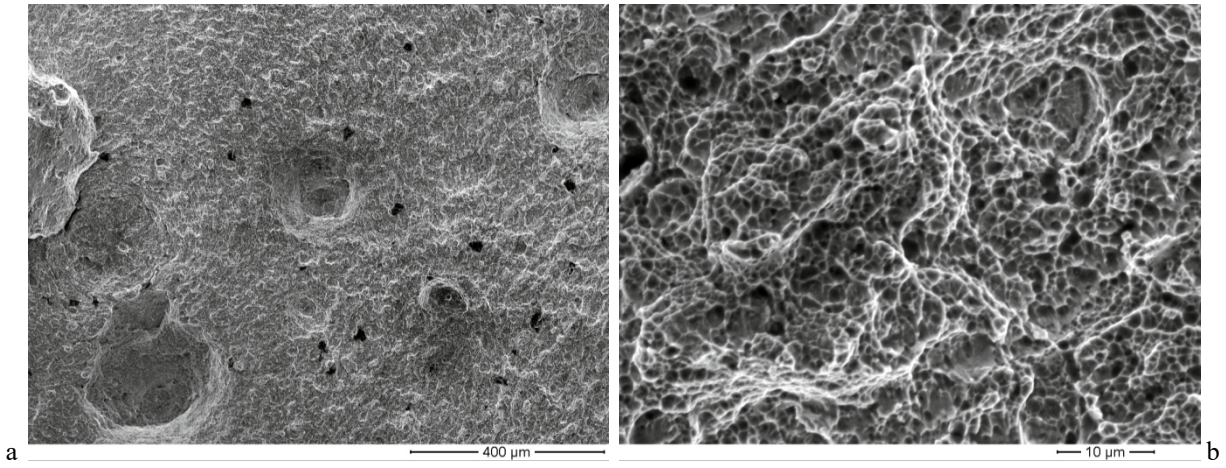

Fig. 6 - Fracture surface of a tensile specimen tempered at 200 °C . Electron microscopy. Central (normal) part. Ductile fracture (prevalent) with brittle islands (a); detail of ductile fracture area (b).

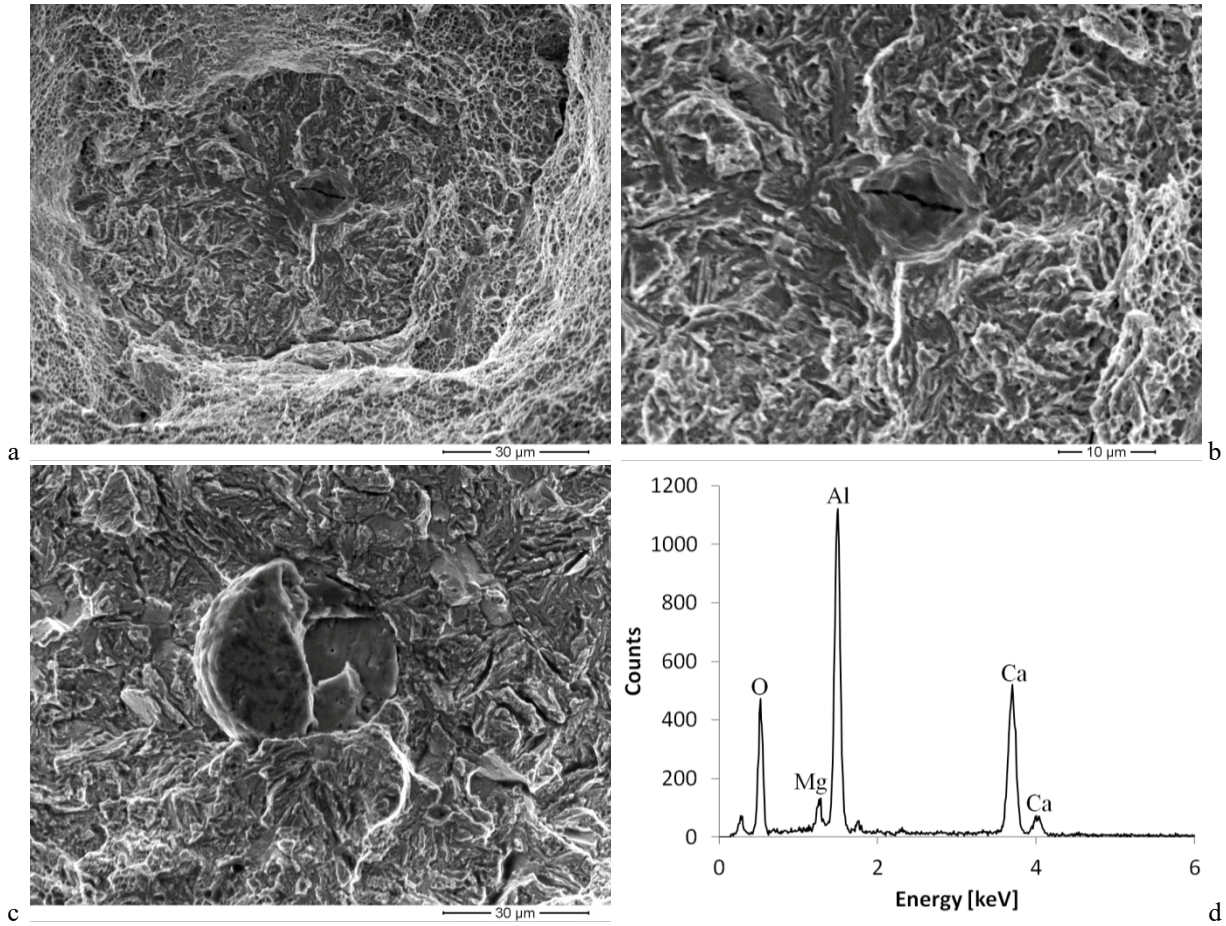

Fig. 7 – Fracture surface of a tensile specimen tempered at 200 °C . Electron microscopy. Central (normal) part. Brittle fracture island (a, b); brittle fracture around a large oxide inclusion (c) and Energy Dispersion Spectroscopy (EDS) analysis of the same inclusion (d).

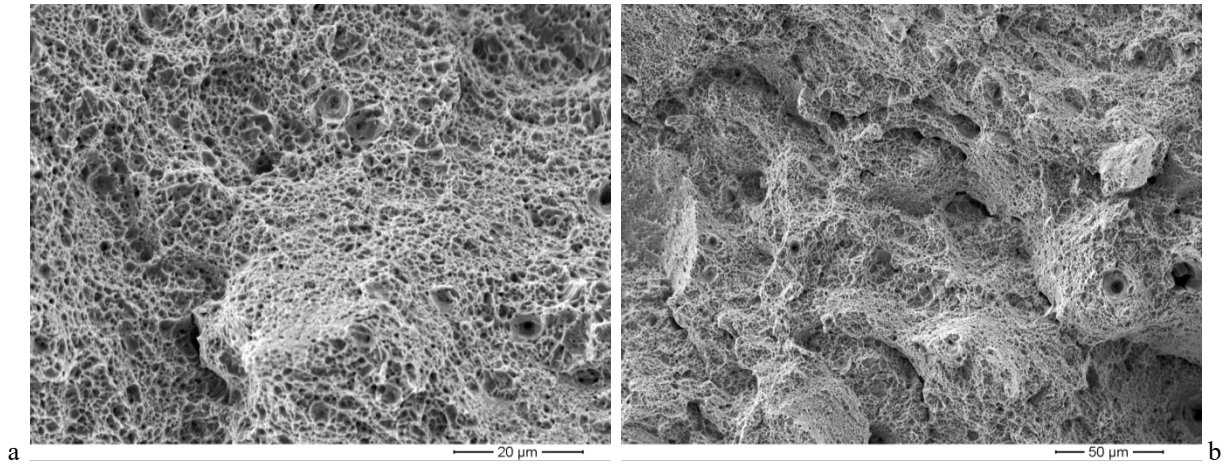

Fig. 8 - Fracture surface of a tensile specimen tempered at 320 °C. Electron microscopy. Central (normal) part. Ductile fracture (a, b).

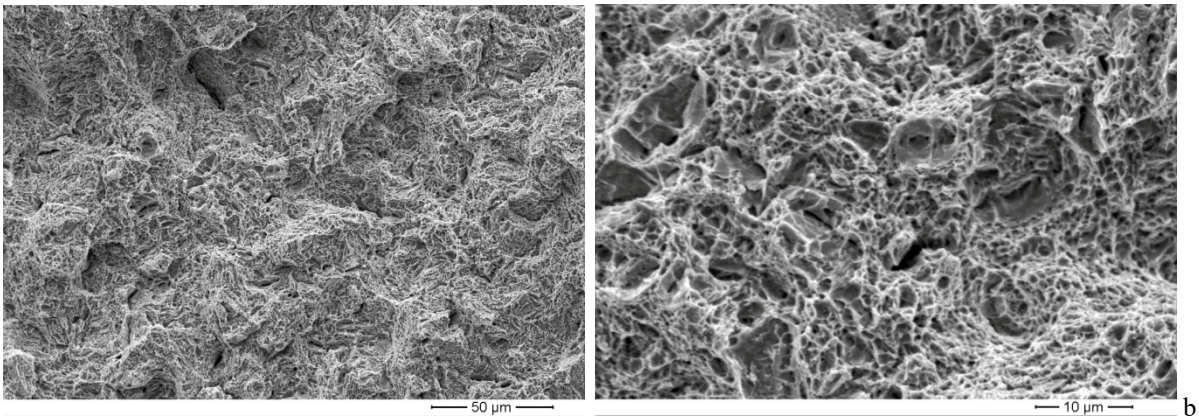

a b

Fig. 9 - Fracture surface of a tensile specimen tempered at 440 °C . Electron microscopy. Central (normal) part. Ductile fracture (a, b).

4. Conclusions

Preliminary results of a research program aiming at the safe employment of conventional medium carbon, low alloy steels in the low tempering temperature regime indicate that, by oil quenching and tempering at 200 °C, UTS values well above 1800 MPa can be reached, while maintaining a 10% elongation-to-fracture.

The here reported tensile test results are overall compatible with data pertaining to another quenched and tempered NiCrMo steel (AISI 4340) (Spretnak and Firrao, 1980; Firrao et al., 1984).

In particular, the here reported tensile test results do not highlight evident signs of temper embrittlement; this fact may be favored by the slightly higher than usual Mo content (0.28% as opposed to 0.2%) of the examined steel.

The origin of the brittle zones on the fracture surfaces, after tempering at 180 and 200 °C, must be further investigated.

References

Averbach B.L., Cohen M., 1949, The isothermal decomposition of martensite and retained austenite, Transactions of the American Society for Metals, vol. 41, 1024-1060.

Borvik T., Dey S., Clausen A.H., 2009, Perforation resistance of five different high-strength steel plates subjected to small-arms projectiles, International Journal of Impact Engineering, vol. 36(7), 948-964.

Cohen M., 1983, Opening of the Peter G. Winchell symposium on the tempering of steel, Metallurgical and Materials Transactions A, vol. 14, 991-993.

Dudzinski, W., Konat L., Pekalski G., 2008, Structural and strength characteristics of wear-resistant martensitic steels, Archives of Foundry Engineering, vol. 8(2), 21-26.

Firrao D., Roberti R., De Benedetti B., 1984, Riflessi del trattamento di austenitizzazione sulla tenacità a frattura dell'acciaio AISI 4340 bonificato, Industria Meccanica, vol. 36, 641-644.

Karbasian, H., Tekkaya, A.E., 2010), A review on hot stamping, Journal of Materials Processing Technology, vol. 210(15), 2103-2118.

Krauss G., 1984, Tempering and structural changes in ferrous martensitic structures, in: Marder A.R., Goldstein J.J. (editors), Phase Transformations in Ferrous Alloys, TMS-AIME, Warrendale, PA, USA, 101-123.

Lee H.C., Krauss G., 1992, Intralath carbide transition in martensitic medium-carbon steelstempered between 200 and 300 °C, in: Fundamentals of Aging and Tempering in Bainitic and Martensitic Steel Products, ISS, Warrendale, PA, USA, 39-43

Mentser M., 1959, Magnetic analysis of phase changes produced in tempering a high carbon steel, Transactions of the American Society for Metals, vol. 51, 517.

Roberts C.S., Averbach B.L., Cohen M., 1953, The mechanism and kinetics of the first stage of tempering, Transactions of the American Society for Metals, vol. 45, 576-604.

Sachs G., Sangdahl G.S., Brown W.F., 1950, New notes on high strength heat-treated steels, Iron Age, Nov. 23, 59-63, and Nov. 30, 76-80.

Spretnak J.W., Firrao D., 1980, Considerazioni sul ruolo dell'instabilità plastica nella formazione di fratture di tipo duttile, Metallurgia Italiana, vol. 72, 525-534.